

Vibrational Stabilization of Cluster Synchronization in Oscillator Networks

YUZHEN QIN ¹ (Member, IEEE), ALBERTO MARIA NOBILI ², DANIELLE S. BASSETT ^{3,4} (Member, IEEE),
AND FABIO PASQUALETTI ⁵ (Member, IEEE)

(Synchronization in Natural and Engineering Systems)

¹Department of Artificial Intelligence, Donders Institute for Brain, Cognition, and Behaviour, Radboud University, 6525 GD Nijmegen, The Netherlands

²Perceptual Robotics Laboratory at the IIM Institute, Department of Excellence in Robotics and A.I., Scuola Superiore Sant'Anna, 56010 Pisa, Italy

³Department of Bioengineering, Department of Electrical and Systems Engineering, Department of Physics and Astronomy, the Department of Psychiatry, and Department of Neurology, University of Pennsylvania, Philadelphia, PA 19104 USA

⁴Santa Fe Institute, Santa Fe, NM 87501 USA

⁵Department of Mechanical Engineering, University of California, Riverside, CA 92521 USA

CORRESPONDING AUTHOR: YUZHEN QIN (e-mail: yuzhen.qin@donders.ru.nl)

This work was supported in part by Aligning Science Across Parkinson's under Grant ASAP-020616, in part by the NSF under Grant NCS-FO-1926829, in part by ARO under Grant W911NF1910360, and in part by Project Dutch Brain Interface Initiative (DBI2) under Project 024.005.022 through Research Programme Gravitation which is (partly) financed by the Dutch Research Council (NWO).

ABSTRACT Cluster synchronization is of great importance for the normal functioning of numerous technological and natural systems. Deviations from normal cluster synchronization patterns are closely associated with various malfunctions, such as neurological disorders in the brain. Therefore, it is crucial to restore normal system functions by stabilizing the appropriate cluster synchronization patterns. Most existing studies focus on designing controllers based on state measurements to achieve system stabilization. However, in many real-world scenarios, measuring system states in real time, such as neuronal activity in the brain, poses significant challenges, rendering the stabilization of such systems difficult. To overcome this challenge, in this article, we employ an open-loop control strategy, *vibrational control*, which does not require any state measurements. We establish some sufficient conditions under which vibrational inputs stabilize cluster synchronization. Further, we provide a tractable approach to design vibrational control. Finally, numerical experiments are conducted to demonstrate our theoretical findings.

INDEX TERMS Cluster synchronization, oscillator networks, vibrational control.

I. INTRODUCTION

Cluster synchronization describes the phenomenon in which units within a network exhibit synchronized behavior, forming distinct clusters. This intriguing phenomenon is widely observed in many natural and engineering systems. For instance, it manifests as correlated neural activity in the brain. Different patterns of cluster synchronization in the brain play a fundamental role in various functions, including neuronal communication, memory formation and retrieval, and motor function [1], [2].

However, many brain disorders, such as Parkinson's disease [3] and epilepsy [4], are characterized by aberrant synchrony patterns of brain activity. It becomes crucial to be able to stabilize normal patterns of cluster synchronization.

Most existing studies rely on the assumption that the states of systems can be measured to design feedback controllers to stabilize them. Unfortunately, many real-world systems often exhibit complex nonlinear dynamics over large network structures with states that are difficult to observe or measure in real time (such as neuronal activity in the brain), thus preventing the use of sophisticated feedback techniques.

In this article we leverage *vibrational control* strategies to ensure stability of network systems. Vibrational control is a powerful strategy applicable in various domains to stabilize the dynamics of complex systems without the need for direct state measurements. Unlike traditional feedback-based control methods that rely on directly measuring the system's states or outputs, vibrational control leverages the

inherent dynamics of the system to induce desired stability and performance. In particular, vibrational control uses pre-designed high-frequency signals, injected at specific locations and times. As we show below, these signals can effectively change the system dynamics and suppress unstable dynamics. Successful applications of vibrational control to individual systems are numerous, including inverted pendulums, chemical reactors, and under-actuated robots [5], [6], [7]. This article takes the first steps to develop a theory of vibrational control for network systems. Interestingly, in addition to its technological value, the theory of vibrational control for network systems may also help explain the success of deep brain stimulation methods, as this technique also relies on the injection of high-frequency electrical pulses to regulate brain processes and restore healthy functions [8].

We study the stabilization of networks of heterogeneous Kuramoto oscillators, and in particular on the stabilization of the dynamics around a desired cluster synchronization manifold [9]. We remark that (i) Kuramoto-oscillator networks have been used successfully to model different phenomena in diverse domains ranging from power engineering to biology and neuroscience, thus making our results of broad applicability, and (ii) cluster synchronization has been used as a proxy to model and regulate the emergence of functional activation patterns in the brain [10], [11], thus making our results of timely relevance to these problems.

Related work: Cluster synchronization has garnered significant attention recently as researchers seek to understand its underlying mechanisms and control strategies. Investigations into the field have revealed intriguing connections between cluster synchronization and network symmetries [12], [13], [14], [15] as well as equitable partitions [16]. Furthermore, stability conditions for cluster synchronization have been established in networks featuring dyadic connections [9], [17], [18], [19], [20] and hyper connections [21], [22]. To control cluster synchronization, researchers have proposed diverse strategies, such as pinning control [23] and interventions that involve manipulating network connections or the dynamics of individual nodes [24], [25], [26]. In contrast, our approach focuses on vibrational control, which offers a more realistic strategy in many real-world systems, e.g., for regulating neural activity as it resembles deep brain stimulation [8]. To the best of our knowledge, our work is among the first ones to utilize vibrations to regulate network systems.

Paper contributions: The main contributions of this article are as follows. First, we formalize the problem of vibrational control for Kuramoto-oscillator networks, with the aim to stabilize patterns of cluster synchronization. By employing an averaging technique, we demonstrate that introducing vibrational inputs into the network effectively alters the system dynamics on average. We establish sufficient conditions for the effectiveness of vibrational control in stabilizing cluster synchronization within Kuramoto-oscillator networks. Through the analysis of linearized systems, we gain deep insights into the underlying mechanisms of vibrational control, revealing its ability to enhance the robustness of synchronization within

clusters. Second, we establish a connection between the design of vibrational control in Kuramoto-oscillator networks and linear network systems. We show that vibrational control can effectively modify the weights of edges in linear network systems, thereby shaping their robustness. We develop graph-theoretical conditions for determining which edges can be modified through vibration. Additionally, we propose a systematic approach to designing vibrational control that targets the modifiable edges, aiming to enhance the overall robustness of the network system. Building on these findings, we apply the results to homogeneous Kuramoto-oscillator networks, presenting a tractable approach to designing vibrational control for improving the robustness of full synchronization. Furthermore, we extend the application of these results to heterogeneous Kuramoto-oscillator networks, deriving precise forms and placements of vibrational inputs to stabilize cluster synchronization. Finally, we conduct a numerical experiment to demonstrate our method for designing vibrational control to stabilize cluster synchronization in Kuramoto-oscillator networks.

A preliminary version of this work appeared in [27]. Compared with it, this article presents a more comprehensive approach to design vibrational control in Kuramoto-oscillator networks by deriving and utilizing precise forms and placements of vibrational inputs in linear network systems.

Notation: Denote the unit circle by \mathbb{S}^1 , and a point on it is called a *phase* since the point can be used to indicate the phase angle of an oscillator. For any two phases $\theta_1, \theta_2 \in \mathbb{S}^1$, the geodesic distance between them is the minimum of the lengths of the counter-clockwise and clockwise arcs connecting them, which is denoted by $|\theta_1 - \theta_2|_{\mathbb{S}}$. Given a matrix $B \in \mathbb{R}^{m \times n}$, the matrix $A = \text{sign}(B)$ is defined in a way such that $a_{ij} = 1$ if $b_{ij} > 0$, $a_{ij} = -1$ if $b_{ij} < 0$, and $a_{ij} = 0$ if $b_{ij} = 0$. Given a matrix A , A^\dagger denote its pseudo-inverse. Given a vector $a \in \mathbb{R}^n$, $\text{diag}(a)$ denotes the diagonal matrix formed by a . Given matrices A_1, A_2, \dots, A_n , $\text{blkdiag}(A_1, A_2, \dots, A_n)$ denotes the block diagonal matrix formed by them. Denote \otimes and \odot as the Kronecker product and point-wise product, respectively.

II. PROBLEM FORMULATION

A. KURAMOTO-OSCILLATOR NETWORKS

Consider a network of n Kuramoto oscillators with dynamics described by

$$\dot{\theta}_i = \omega_i + \sum_{j=1}^n w_{ij} \sin(\theta_j - \theta_i), \quad (1)$$

where $\theta_i \in \mathbb{S}^1$ is the phase of the i th oscillator, $\omega_i \in \mathbb{R}$ is its natural frequency for $i = 1, \dots, n$, and w_{ij} is the coupling strength. This article investigates a network configuration where connections between nodes are bidirectional but allow for asymmetry (i.e., $w_{ji} \neq 0$ if $w_{ij} \neq 0$, and $w_{ij} \neq w_{ji}$ is allowed). This assumption represents a more flexible scenario compared to the commonly studied undirected networks in existing literature. We use a weighted directed graph

$\mathcal{G} = (\mathcal{V}, \mathcal{E}, W)$ to describe the network structure, where $\mathcal{V} = \{1, 2, \dots, n\}$, $\mathcal{E} \subseteq \mathcal{V} \times \mathcal{V}$, and $W = [w_{ij}]_{n \times n}$ with $w_{ij} \geq 0$ is the weighted adjacency matrix. There is a directed edge from j to i in \mathcal{G} , i.e., $(j, i) \in \mathcal{E}$, if $w_{ij} > 0$; this edge does not exist, i.e., $(j, i) \notin \mathcal{E}$, if $w_{ij} = 0$.

In this article, we are interested in studying cluster synchronization in the Kuramoto-oscillator network (1). Let us first formally define cluster synchronization.

For the graph $\mathcal{G} = (\mathcal{V}, \mathcal{E}, W)$, consider the partition of the nodes in it below:

$$\mathcal{P} := \{\mathcal{P}_1, \mathcal{P}_2, \dots, \mathcal{P}_r\}, \quad (2)$$

where each \mathcal{P}_k is a subset of \mathcal{V} satisfying $\mathcal{P}_k \cap \mathcal{P}_\ell = \emptyset$ for any $k \neq \ell$, and $\bigcup_{k=1}^r \mathcal{P}_k = \mathcal{V}$.

Definition 1 (Cluster Synchronization Manifold): The cluster synchronization manifold with respect to the partition \mathcal{P} is defined as

$$\mathcal{M} := \{\theta \in \mathbb{T}^n : \theta_i = \theta_j, \forall i, j \in \mathcal{P}_k, k = 1, \dots, r\}. \quad \Delta$$

Note that various cluster synchronization patterns may emerge in the same network, each of which corresponds to a distinct network partition. Nevertheless, the partition defined in (2) exhibits sufficient generality to capture any cluster synchronization pattern, enabling the analysis of different patterns of cluster synchronization.

The manifold \mathcal{M} is invariant along the system (1) if, starting from $\theta(0) \in \mathcal{M}$, the solution to (1) satisfies $\theta(t) \in \mathcal{M}$ for all $t \geq 0$. We make the following assumption to ensure the invariance of \mathcal{M} .

Assumption 1 (Invariance): For $k = 1, 2, \dots, r$: i) the natural frequencies satisfy $\omega_i = \omega_j$ for any $i, j \in \mathcal{P}_k$; and ii) the coupling strengths satisfy that, for any $\ell \in \{1, 2, \dots, r\} \setminus \{k\}$, $\sum_{q \in \mathcal{P}_\ell} (w_{iq} - w_{jq}) = 0$ for any $i, j \in \mathcal{P}_k$. Δ

This assumption guarantees that oscillators within a cluster receive identical inputs from every other synchronized cluster, a critical factor for maintaining synchronization among them. Similar assumptions are made for undirected networks in earlier studies [9], [28]. To ensure the emergence of cluster synchronization, it is essential to not only establish invariance but also ensure the stability of \mathcal{M} . Given a manifold $\mathcal{C} \in \mathbb{T}^n$, define a δ -neighborhood of \mathcal{C} by $U_\delta(\mathcal{C}) = \{\theta \in \mathbb{T}^n : \text{dist}(\theta, \mathcal{C}) < \delta\}$ with $\text{dist}(\theta, \mathcal{C}) = \inf_{y \in \mathcal{C}} \|\theta - y\|_S$. The exponential stability of the manifold \mathcal{M} is defined below.

Definition 2: The manifold $\mathcal{M} \in \mathbb{T}^n$ is said to be exponentially stable along the system (1) if there is $\delta > 0$ such that for any initial phase $\theta(0) \in \mathbb{T}^n$ satisfying $\theta(0) \in U_\delta(\mathcal{M})$ it holds that for all $t \geq 0$, $\text{dist}(\theta(t), \mathcal{M}) = k \cdot \text{dist}(\theta(0), \mathcal{C}) \cdot e^{-\lambda t}$ for some $k > 0$ and $\lambda > 0$.

Sufficient conditions are constructed for the exponential stability of \mathcal{M} (e.g., see [9], [16], [17]). However, variations in network parameters due to factors, e.g., aging or brain disorders, can disrupt such conditions, resulting in the loss of stability of cluster synchronization. This article focuses on the application of *vibrational control*, a control strategy reminiscent of deep brain stimulation (DBS) [8], to restore

the stability of desired cluster synchronization patterns. Next, we present an introduction to vibrational control.

B. VIBRATIONAL CONTROL

Following [29], consider a nonlinear system

$$\dot{x} = f(x, a), \quad (3)$$

where $x \in \mathbb{R}^n$, and $a \in \mathbb{R}^m$ represents the parameters of the system. For linear systems, a can be rewritten into a matrix form $A \in \mathbb{R}^{n \times n}$, and then we have $\dot{x} = Ax$. Vibrational control introduces vibrations to the parameters of (3), resulting in

$$\dot{x} = f(x, a + v(t)). \quad (4)$$

The control vector $v(t) = [v_1, v_2, \dots, v_m]^T \in \mathbb{R}^m$ is usually selected to have the following structure:

$$v_i(t) = \sum_{\ell=1}^{\infty} \alpha_i^{(\ell)} \sin(\ell \beta_i t + \varphi_i^{(\ell)}). \quad (5)$$

which is almost-periodic, zero-mean, and high-frequency [5]. Vibrational control is an open-loop strategy. An appropriate configuration of vibrations can stabilize an unstable system (3) without any measurements of the states [6], [7], [30].

C. VIBRATIONAL CONTROL IN KURAMOTO-OSCILLATOR NETWORKS

In the Kuramoto-oscillator network described by (1), the natural frequencies and coupling strengths can be taken as the parameters. This article specifically focuses on injecting vibrations solely into the network connections, affecting their coupling strengths (i.e., the strengths of edges in the associated graph). This is inspired by the observation that deep brain stimulation predominantly affects dendrites and axons near the electrode, rather than the soma [31].

The control inputs exert their influence on the system in the way specified by

$$\dot{\theta}_i = \omega_i + \sum_{j=1}^n (w_{ij} + v_{ij}(t)) \sin(\theta_j - \theta_i), \quad (6)$$

where $v_{ij}(t)$ is the vibration introduced to the edge (j, i) . Particularly, we consider that each $v_{ij}(t)$ is simply sinusoidal, which naturally satisfies (5), i.e.,

$$v_{ij}(t) = \mu_{ij} \sin(\alpha_{ij} t), \quad (7)$$

Let $V(t) = [v_{ij}(t)]_{n \times n}$. Note that various types of vibrations can be utilized in practical applications. However, for the sake of analysis simplification, we just consider sinusoidal vibrations in this article. Here, $\mu_{ij} \in \mathbb{R}$ and $\alpha_{ij} > 0$ determine the amplitude and frequency of the vibration injected to the connection (i, j) . Note that, since vibrations are usually high-frequency, μ_{ij} and α_{ij} are often rewritten into the form of $\mu_{ij} = u_{ij}/\varepsilon$ and $\alpha_{ij} = \beta_{ij}/\varepsilon$ to streamline the analysis, where u_{ij} and β_{ij} have the order of 1, and $\varepsilon > 0$ is a small constant. Let $u_{ij}(t) = u_{ij} \sin(\beta_{ij} t)$, and $v_{ij}(t)$ can be rewritten as $v_{ij}(t) = \frac{1}{\varepsilon} u_{ij}(\frac{t}{\varepsilon})$.

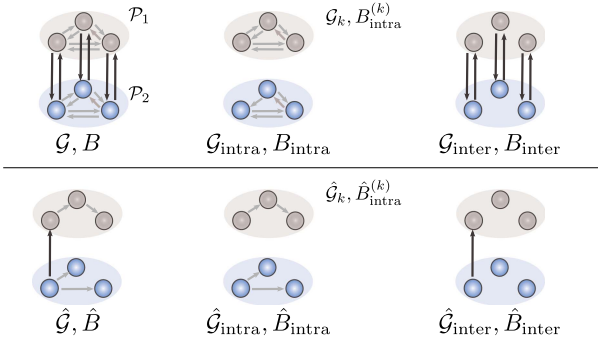


FIGURE 1. Summary of the main notations we use in this article: different subgraphs and their corresponding incidence matrices.

In contrast to the general system (3), where vibrations can be applied to any parameter in a , the introduction of vibrational control to a network system is subject to the constraints imposed by the network structure. It is reasonable to assume that vibrations can only be introduced to connections that already exist in the network. Therefore, vibrational control satisfies that for any pair of i, j ,

$$u_{ij} = 0, \quad \text{if } w_{ij} = 0. \quad (8)$$

Objective: This article aims to study how vibrational control satisfying both (7) and (8) stabilizes the cluster synchronization represented by the manifold \mathcal{M} .

III. PRELIMINARY

A. GRAPH-THEORETICAL NOTATIONS

We first introduce some graph-theoretical notations, which are further elucidated in a more intuitive manner in Fig. 1.

For the directed graph $\mathcal{G} = (\mathcal{V}, \mathcal{E}, W)$ that describes the network in (1), denote the oriented incidence matrix as $B = [b_{k\ell}] \in \mathbb{R}^{n \times m}$, where

$$b_{k\ell} = \begin{cases} -1, & \text{if the edge } e_\ell \text{ leave the node } k, \\ 1, & \text{if the edge } e_\ell \text{ enters the node } k, \\ 0, & \text{otherwise.} \end{cases}$$

For the partition $\mathcal{P} := \{\mathcal{P}_1, \mathcal{P}_2, \dots, \mathcal{P}_r\}$ of \mathcal{G} , define $\mathcal{G}_k = (\mathcal{P}_k, \mathcal{E}_k)$ where $\mathcal{E}_k := \{(i, j) \in \mathcal{E} : i, j \in \mathcal{P}_k\}$ for all $k = 1, \dots, r$. Denote $n_k := |\mathcal{P}_k|$ as the number of nodes in \mathcal{G}_k . We assume that each \mathcal{G}_k contains at least 2 nodes and is strongly connected. Let $\mathcal{G}_{\text{intra}} = (\mathcal{V}, \mathcal{E}_{\text{intra}}) = \cup_{k=1}^r \mathcal{G}_k$, and we refer to it as the *intra-cluster subgraph*, describing the intra-cluster network structure. Similarly, let $\mathcal{G}_{\text{inter}} = (\mathcal{V}, \mathcal{E}_{\text{inter}})$ be the *inter-cluster subgraph*, where $\mathcal{E}_{\text{inter}} := \mathcal{E} \setminus \mathcal{E}_{\text{intra}}$. Denote B_{intra} and B_{inter} as the oriented incidence matrices of $\mathcal{G}_{\text{intra}}$ and $\mathcal{G}_{\text{inter}}$, respectively.

Consider an arbitrary spanning tree in \mathcal{G} , and denote it by $\hat{\mathcal{G}} = (\mathcal{V}, \hat{\mathcal{E}})$, where $|\hat{\mathcal{E}}| = n - 1$. Let \hat{B} be the oriented incidence matrix of $\hat{\mathcal{G}}$. For each k , Let $\hat{\mathcal{G}}_k = (\mathcal{P}_k, \hat{\mathcal{E}}_k)$ with $\hat{\mathcal{E}}_k := \hat{\mathcal{E}} \cap \mathcal{E}_k$. Similar to earlier notations, denote the intra-cluster subgraph of the spanning tree $\hat{\mathcal{G}}$ by $\hat{\mathcal{G}}_{\text{intra}} = (\mathcal{V}, \hat{\mathcal{E}}_{\text{intra}}) := \cup_{k=1}^r \hat{\mathcal{G}}_k$; the inter-cluster subgraph of $\hat{\mathcal{G}}$ is denoted by $\hat{\mathcal{G}}_{\text{inter}} =$

$(\mathcal{V}, \hat{\mathcal{E}}_{\text{inter}})$ with $\hat{\mathcal{E}}_{\text{inter}} := \hat{\mathcal{E}} \setminus \hat{\mathcal{E}}_{\text{intra}}$. Denote the incidence matrices of $\hat{\mathcal{G}}_{\text{intra}}$ and $\hat{\mathcal{G}}_{\text{inter}}$ as $\hat{B}_{\text{intra}} \in \mathbb{R}^{n \times (n-r)}$ and $\hat{B}_{\text{inter}} \in \mathbb{R}^{n \times (r-1)}$, respectively.

B. INCREMENTAL DYNAMICS AND PARTIAL STABILITY

To study cluster synchronization in (6), we look at its incremental dynamics. Specifically, we order the columns of the incidence matrix \hat{B} of the spanning tree $\hat{\mathcal{G}}$ in a way such that $\hat{B} = [\hat{B}_{\text{intra}}, \hat{B}_{\text{inter}}]$, where $\hat{B}_{\text{intra}} \in \mathbb{R}^{n \times (n-r)}$ and $\hat{B}_{\text{inter}} \in \mathbb{R}^{n \times (r-1)}$ represents the intra- and inter-cluster subnetwork in the spanning tree $\hat{\mathcal{G}}$, respectively. Now, let $x = \hat{B}_{\text{intra}}^\top \theta \in \mathbb{R}^{n-r}$ and $y = \hat{B}_{\text{inter}}^\top \theta \in \mathbb{R}^{r-1}$ to capture intra- and inter-cluster phase differences, respectively. Naturally, $x = 0$ implies the cluster synchronization defined by \mathcal{M} since it indicates that phase differences of oscillators within each cluster are all 0.

Now, the incremental dynamics of the Kuramoto-oscillator network can be derived as

$$\dot{x} = f_{\text{intra}}(x) + f_{\text{inter}}(x, y) + h_{\text{ctl}} \left(\frac{1}{\varepsilon} \mathbf{U} \left(\frac{t}{\varepsilon} \right), x, y \right), \quad (9a)$$

$$\dot{y} = g(x, y) + h'_{\text{ctl}} \left(\frac{1}{\varepsilon} \mathbf{U} \left(\frac{t}{\varepsilon} \right), x, y \right), \quad (9b)$$

where $\mathbf{U}(t) = \text{diag}([u_{ij}(t)]_{(i,j) \in \mathcal{E}}) \in \mathbb{R}^{m \times m}$ captures the vibrations introduced to the edges in the network. The expressions of the functions on the right-hand side of (9) are given in Appendix A. We single out some important properties of them. The functions f_{intra} and f_{inter} results from intra- and inter-cluster couplings; it holds that $f_{\text{intra}}(0) = 0$ and $f_{\text{inter}}(0, y) = 0$ for any y . The functions h_{ctl} and h'_{ctl} are the consequences of vibrational inputs; when there is no control, $h_{\text{ctl}}(0, x, y) = 0$ and $h'_{\text{ctl}}(0, x, y) = 0$ for any x, y .

Notice that, the fact that $f_{\text{intra}}(x) + f_{\text{inter}}(x, y) = 0$ when $x = 0$ signifies the invariance of cluster synchronization defined by \mathcal{M} . To preserve this invariance, a vibrational control input needs to ensure $h_{\text{ctl}}(\frac{1}{\varepsilon} \mathbf{U}(\frac{t}{\varepsilon}), 0, y) = 0$ for any y . To meet this requirement, one way is to assume a similar balanced condition as Assumption 1, that is, one can consider that, given any ℓ and k , it holds for all $t \geq 0$ that

$$\sum_{q \in \mathcal{P}_\ell} (u_{iq}(t) - u_{jq}(t)) = 0 \text{ for any } i, j \in \mathcal{P}_k. \quad (10)$$

This assumption ensures that $x = 0$ is an equilibrium of the system (9a), independent of y . Following [32, Chap. 4], such an equilibrium is called a *partial equilibrium* of the system (9). To ensure the stability of the cluster synchronization manifold \mathcal{M} , one can focus on the stability of the partial equilibrium $x = 0$ of the system (9), which reduces to studying its partial stability. Note that various forms of partial stability exist, such as partial asymptotic and exponential stability, as elaborated in [32, Chap. 4]. However, for the scope of our discussion, we exclusively focus on partial exponential stability and therefore present its specific definition here.

Definition 3 (Partial Exponential Stability [32, Chap. 4]): Given a system $\dot{x} = f(x, y), \dot{y} = g(x, y)$, where $x \in \mathbb{R}^n, y \in \mathbb{R}^m$, a partial equilibrium point $x = 0$ is *exponentially x -stable*

uniformly in y if there exist $c_1, c_2, \delta > 0$ such that $\|x(0)\| < \delta$ and any $y(0) \in \mathbb{R}^m$ imply that $\|x(t)\| \leq c_1 \|x_0\| e^{-c_2 t}$ for all $t \geq 0$.

Formally, the manifold \mathcal{M} is exponentially stable along the system (6) if $x = 0$ of the system (12) is partially exponentially stable. To stabilize the cluster synchronization manifold \mathcal{M} , it suffices to design vibration control satisfying (10) to ensure the partial exponential stability of $x = 0$.

IV. VIBRATIONAL STABILIZATION: GENERAL RESULTS

In this article, we specifically investigate a form of vibrational control in which vibrations are exclusively introduced to the intra-cluster connections, i.e.,

$$u_{ij}(t) = 0, \quad (11)$$

for any i, j from different clusters. Then, the requirement (10) is naturally met since $\sum_{q \in \mathcal{P}_\ell} u_{iq}(t) = 0$ for any i . As a result, the system (9) reduces to (see details in Appendix A)

$$\dot{x} = f_{\text{intra}}(x) + f_{\text{inter}}(x, y) + \frac{1}{\varepsilon} h_{\text{ctl}} \left(U \left(\frac{t}{\varepsilon} \right), x \right), \quad (12a)$$

$$\dot{y} = g(x, y) + \frac{1}{\varepsilon} h'_{\text{ctl}} \left(U \left(\frac{t}{\varepsilon} \right), x \right), \quad (12b)$$

where h_{ctl} and h'_{ctl} no longer depend on y .

Since $f_{\text{inter}}(0, y) = 0$ holds for any y , then the term $f_{\text{inter}}(x, y)$ in (12a) can be viewed as a vanishing perturbation dependent of y to the controlled nominal system

$$\dot{x} = f_{\text{intra}}(x) + \frac{1}{\varepsilon} f_{\text{ctl}} \left(U \left(\frac{t}{\varepsilon} \right), x \right). \quad (13)$$

This perturbation can be decomposed as

$$f_{\text{inter}} = [(f_{\text{inter}}^{(1)})^\top, \dots, (f_{\text{inter}}^{(r)})^\top]^\top$$

where $f_{\text{inter}}^{(k)} = -(\hat{B}_{\text{intra}}^{(k)})^\top \mathbb{B}_{\text{inter}} \mathbf{W}_{\text{inter}} \sin(R_2 x + R_3 y)$ is the perturbation received by the k th cluster.¹

Next, we show how a vibration control can stabilize $x = 0$ in the presence of the perturbation $f_{\text{inter}}(x, y)$ by introducing the change $\frac{1}{\varepsilon} f_{\text{ctl}}(U, x)$ to the system dynamics.

To this end, we linearize the system at $x = 0$ and obtain

$$\dot{\bar{x}} = \left(J + \frac{1}{\varepsilon} P \left(\frac{t}{\varepsilon} \right) \right) \bar{x} + N(y) \bar{x}, \quad (14)$$

where

$$\begin{aligned} J &= \frac{\partial f_{\text{intra}}}{\partial x}(0) = \text{blkdiag}(J^{(1)}, \dots, J^{(r)}), \\ P(t) &= \frac{\partial f_{\text{ctl}}}{\partial x}(0, t) = \text{blkdiag}(P^{(1)}(t), \dots, P^{(r)}(t)), \\ N(y) &= \frac{\partial f_{\text{inter}}}{\partial x}(0, y). \end{aligned} \quad (15)$$

¹The matrix \mathbb{B} is obtained by replacing the negative elements in the oriented incidence matrix B with 0. The columns of \mathbb{B} can be ordered such that $\mathbb{B} = [\mathbb{B}_{\text{intra}}, \mathbb{B}_{\text{inter}}]$ and $\mathbb{B}_{\text{intra}} = [\mathbb{B}_{\text{intra}}^{(1)}, \mathbb{B}_{\text{intra}}^{(2)}, \dots, \mathbb{B}_{\text{intra}}^{(r)}]$. The diagonal matrix $\mathbf{W} = \text{blkdiag}(\mathbf{W}_{\text{intra}}, \mathbf{W}_{\text{inter}}) := \text{diag}([w_{ij}]_{(i,j) \in \mathcal{E}})$ contains the weights, and the matrices R_1, R_2 , and R_3 capture the relation between θ and x, y . More details can be found in Appendix A.

Notice that both J and $P(t)$ are block-diagonal, because the dynamics described by f_{intra} and the vibrational control f_{ctl} have no inter-cluster couplings. Here, for each k , $J^{(k)} = -(\hat{B}_{\text{intra}}^{(k)})^\top \mathbb{B}_{\text{intra}}^{(k)} \mathbf{W}_{\text{intra}}^{(k)} R_1$ and $P^{(k)}(t) = -(\hat{B}_{\text{intra}}^{(k)})^\top \mathbb{B}_{\text{intra}}^{(k)} U^{(k)}(t) R_1$. One can also derive that

$$N(y) = -(\hat{B}_{\text{intra}})^{\top} \mathbb{B}_{\text{inter}} \mathbf{W}_{\text{inter}} (\mathbb{1}_{n-r}^\top \otimes \sin(R_3 y)) \odot R_2.$$

Observe that $P(t)$ is almost periodic with a zero mean value just as $U(t)$. Different from our previous work [27], here we also linearize the perturbation $f_{\text{inter}}(x, y)$ at $x = 0$ in (14).

Lemma 1 (Connecting the stability of Systems (12) and (14)): If the equilibrium $\bar{x} = 0$ of the system (14) is exponentially stable uniformly in y , then $x = 0$ of the system (12) is also exponentially stable uniformly in y .

From this lemma, a vibrational control resulting in $P(t)$ that stabilizes $x = 0$ of the system (14) stabilizes the cluster synchronization manifold \mathcal{M} , too. Next, we aim to provide conditions on which a vibrational control stabilizes the system (14).

Let $s = t/\varepsilon$, then we rewrite the system (14) as

$$\frac{d\bar{x}}{ds} = (\varepsilon J + P(s)) \bar{x} + \varepsilon N(y) \bar{x}. \quad (16)$$

Next, we use averaging methods to analyze this system. However, the standard first-order averaging² is not applicable here. Recall that $P(s)$ has zero mean. Then, applying the first-order averaging to (16) just eliminates the $P(s)$ term and results in the uncontrolled system $\frac{d\bar{x}}{ds} = \varepsilon J \bar{x} + \varepsilon N(y) \bar{x}$.

To avoid that, we change the coordinates of (16) first before using the averaging method. To do that, we introduce an auxiliary system

$$\frac{d\hat{x}}{ds} = P(s) \hat{x}, \quad (17)$$

and let $\Phi(s, s_0)$ be its state transition matrix. Since P is block-diagonal, it holds that $\Phi = \text{blkdiag}(\Phi^{(1)}, \dots, \Phi^{(r)})$, where $\Phi^{(k)}$ is the transition matrix of the subsystem in the k th cluster $d\hat{x}_k/ds = P^{(k)}(s) \hat{x}_k$.

Consider the change of coordinates $z(s) = \Phi^{-1}(s, s_0) \bar{x}(s)$. It follows from the system (16) that

$$\frac{dz}{ds} = \varepsilon \Phi^{-1} J \Phi z + \varepsilon \Phi^{-1} N(y) \Phi z. \quad (18)$$

Since $P(s)$ is almost periodic in s and mean-zero, so are $\Phi(s, s_0)$ and $\Phi^{-1}(s, s_0)$. Denote

$$G(y) := \Phi^{-1} N(y) \Phi.$$

For each $k = 1, \dots, r$, let $G^{(k)}(y) \in \mathbb{R}^{(n_i-1) \times n_i}$ be the dynamics associated with the k th cluster. Now, we associate (18) with a partially averaged system

$$\frac{dz}{ds} = \varepsilon (\bar{J} + G(y)) z, \quad (19)$$

²Given a system $\dot{x} = \varepsilon f(t, x) + \varepsilon^2 h(t, x) + \dots + \varepsilon^k g(t, x)$, the first averaging method calculates the averaged system $\dot{x} = \varepsilon \bar{f}(t, x)$ only using the first-order term $\varepsilon f(t, x)$ and ignoring the higher-order terms $\mathcal{O}(\varepsilon^2)$, i.e., $\bar{f}(x) = \lim_{T \rightarrow \infty} \frac{1}{T} \int_{t=0}^T f(t, x) dt$ [33].

where

$$\bar{J} = \lim_{T \rightarrow \infty} \frac{1}{T} \int_{s_0}^{s_0+T} \Phi^{-1}(s, s_0) J \Phi(s, s_0) ds. \quad (20)$$

As both J and Φ are block-diagonal, one can derive that \bar{J} is also block-diagonal satisfying $\bar{J} = \text{blkdiag}(\bar{J}^{(1)}, \dots, \bar{J}^{(r)})$ with

$$\bar{J}^{(k)} = \lim_{T \rightarrow \infty} \frac{1}{T} \int_{s_0}^{s_0+T} \left(\Phi^{(k)}(s, s_0) \right)^{-1} J^{(k)} \Phi^{(k)}(s, s_0) ds. \quad (21)$$

Therefore, it holds that

$$\frac{dz^{(k)}}{ds} = \varepsilon \left(\bar{J}^{(k)} z_k + G^{(k)}(y) z \right),$$

Then, it can be shown that for any k , there exist $\bar{\gamma}_{k\ell} > 0$, $\ell = 1, \dots, r$, such that

$$\left\| G^{(k)}(y) z \right\| \leq \sum_{\ell=1}^r \bar{\gamma}_{k\ell} \|z_\ell\|$$

for each k (see Lemma 4 in Appendix A for more details).

Theorem 1 (Sufficient condition for vibrational stabilization): Assume that $\bar{J} = \text{blkdiag}(\bar{J}^{(1)}, \dots, \bar{J}^{(r)})$ in Eq. (20) is Hurwitz. Let \bar{X}_k be the solution to the Lyapunov equation

$$(\bar{J}^{(k)})^\top \bar{X}_k + \bar{X}_k \bar{J}^{(k)} = -I. \quad (22)$$

Define the matrix $S = [s_{k\ell}]_{r \times r}$ with

$$s_{k\ell} = \begin{cases} \lambda_{\max}^{-1}(\bar{X}_k) - \bar{\gamma}_{kk}, & \text{if } k = \ell, \\ -\bar{\gamma}_{k\ell}, & \text{if } k \neq \ell, \end{cases} \quad (23)$$

where $\lambda_{\max}(\cdot)$ denotes the maximum eigenvalue of a matrix. If S is an M -matrix,³ then there exists $\varepsilon^* > 0$ such that, for any $\varepsilon < \varepsilon^*$:

- i) the equilibrium $x = 0$ of the system (12) is exponentially stable uniformly in y ;
- ii) the cluster synchronization manifold \mathcal{M} of the system (6) is exponentially stable.

Note that a similar theorem was presented in our preliminary work [27]. Here, our results are built on a complete instead of a partial linearization technique in (14). Theorem 1 provides a sufficient condition for vibrational control inputs to stabilize the cluster synchronization. To design an effective vibrational control law that stabilizes \mathcal{M} , one can design vibrations to satisfy the following three conditions: i) \bar{J} in (20) is Hurwitz, ii) S defined in (23) is an M -matrix, and iii) the frequency of the vibrations is sufficiently high.

Connections with robustness of linear systems: Consider a stable linear system

$$\dot{x} = Ax.$$

Some earlier works (e.g., [35], [36]) utilize

$$\mathcal{R}(A) := \lambda_{\max}^{-1}(X) \quad (24)$$

³A real non-singular matrix $A = [a_{ij}]$ is an M -matrix if $a_{ij} \leq 0$ for any $i \neq j$, and all its leading principal minors are positive [34, ch. 2.5].

to measure its robustness ($\lambda_{\max}(\cdot)$ stands for the maximum eigenvalue of a matrix), where X is the solution to the Lyapunov equation:

$$A^\top X + XA = -I.$$

A larger $\mathcal{R}(A)$ means that the system is more robust.

In our case, from (14), the uncontrolled intra-dynamics around \mathcal{M} are described by the linearized system

$$\dot{x}_k = J^{(k)} x_k + f_{\text{inter}}^{(k)}(x, y), \quad k = 1, \dots, r, \quad (25)$$

where $J^{(k)}$ is stable and $f_{\text{inter}}^{(k)}(x, y)$ is taken as the vanishing perturbation. Here, $x_k = 0$ means synchronization of the oscillators in the k th cluster. Similarly, one can interpret that $\mathcal{R}(J^{(k)})$ measures the robustness of synchronization in the k th cluster. If the intra-cluster synchronization is sufficiently robust (i.e., $\mathcal{R}(J^{(k)})$'s are sufficiently large) to dominate the perturbations resulted from inter-cluster connections, the cluster synchronization is stable. A sufficient condition is constructed in [9, Th. 3.2]. By contrast, if $\mathcal{R}(J^{(k)})$'s are not large enough, the cluster synchronization can lose its stability. Yet, the robustness of the intra-cluster synchronization can be reshaped by introducing vibrations to the local network connections. The new robustness is instead measured by $\mathcal{R}(\bar{J}^{(k)})$ defined in (21).

Now, the question naturally arises: how to design vibrational control such that the robustness in the cluster can be improved? We aim to provide answers in the next section.

V. IMPROVING ROBUSTNESS BY VIBRATIONAL CONTROL

The primary objective of this section is to demonstrate the design of vibrational control with the intention of enhancing the robustness of synchronization within each cluster. As observed in the concluding part of the previous section, the robustness is intimately linked to the linearized systems of both the uncontrolled system and the averaged controlled system. Hence, we commence by examining the linear system and subsequently explore the applicability of the findings from linear systems to Kuramoto-oscillator networks.

A. LINEAR SYSTEMS

Let us consider a linear system

$$\dot{x} = Ax, \quad (26)$$

where $x \in \mathbb{R}^n$, $A \in \mathbb{R}^{n \times n}$, and A is assumed to be Hurwitz. Consider a vibrational control matrix $U(t)$ that influences the system parameters in A , resulting in the following controlled system

$$\dot{x} = \left(A + \frac{1}{\varepsilon} U \left(\frac{t}{\varepsilon} \right) \right) x, \quad (27)$$

where $U(t) = [u_{ij}(t)]_{n \times n}$ with $u_{ij}(t) = u_{ij} \sin(\beta_{ij} t)$, and $\varepsilon > 0$ is small, determining the frequencies of the vibrations.

Vibrational control can improve the robustness of a stable system. To show this, we follow similar step as in Section IV

to associate (27) with the averaged system

$$\dot{\bar{x}} = \bar{A}\bar{x}, \quad (28)$$

where the time scale has been restored to $t = \varepsilon s$,

$$\bar{A} = \lim_{T \rightarrow \infty} \frac{1}{T} \int_{t=0}^T \Phi^{-1}(t, t_0) A \Phi(t, t_0) dt,$$

and $\Phi(t, t_0)$ is the state transition matrix of the system

$$\dot{\hat{x}} = U(t)\hat{x}. \quad (29)$$

When \bar{A} is Hurwitz, the controlled system (27) behaves like (28) in average if ε is small. Then, one can interpret that vibrational control changes the system matrix from A to \bar{A} in an in-average sense. Vibrational inputs can be designed to carefully modify the elements in A so that $\mathcal{R}(\bar{A})$ is larger than $\mathcal{R}(A)$ to improve robustness.

However, which elements in A and how they can be changed is a challenging problem. An earlier attempt has been made in [30]. Here, we aim to generalize their result by utilizing graph-theoretical approaches.

Specifically, we associate the uncontrolled system $\dot{x} = Ax$ with a weighted directed network $\mathcal{G}_A = (\mathcal{V}, \mathcal{E}_A, A)$. Here, $\mathcal{V} = \{1, 2, \dots\}$, and there is a directed edge from i to j , i.e., $(i, j) \in \mathcal{E}_A$ if $a_{ji} \neq 0$ and $i \neq j$ (no self-loops are considered). The matrix A becomes the weighted adjacency matrix. Likewise, one can associate the averaged controlled system (28) with a weighted directed network $\mathcal{G}_{\bar{A}} = (\mathcal{V}, \mathcal{E}_{\bar{A}}, \bar{A})$, which we refer to as the *functioning network*⁴. Then, changing elements in A reduces to altering the connection weights in \mathcal{G}_A via vibrational control.

Definition 4: The edge $(i, j) \in \mathcal{E}_A$ is said to be vibrationally increasable if there exists a vibrational control $U(t)$ such that the weight of (i, j) is increased in $\mathcal{E}_{\bar{A}}$, i.e., $\bar{a}_{ji} > a_{ji}$. It is said to be vibrationally decreasable if there exists a vibrational control $U(t)$ such that the weight of (i, j) is decreased in $\mathcal{E}_{\bar{A}}$, i.e., $\bar{a}_{ji} < a_{ji}$.

Lemma 2: Consider an edge $(i, j) \in \mathcal{E}_A$. It is vibrationally increasable if there is an edge in the reverse direction that has a negative weight, i.e., $a_{ij} < 0$. It is vibrationally decreasable if there is an edge in the reverse direction that has a positive weight, i.e., $a_{ij} > 0$.

An illustration of vibrationally increasable and decreasable edges can be found in Fig. 2. When an edge satisfies the corresponding conditions, we further find that directly injecting a vibration to it can functionally increase or decrease its weight (see Appendix A for more details).

The conditions we identified here are just sufficient ones. Edges that do not satisfy these conditions may also be vibrationally increasable or decreasable. Yet, we restrict our attention to the edges that satisfy the conditions in Lemma 2. Then, based on them, we define two sets $\mathcal{E}_{\text{inc}} := \{(i, j) \in$

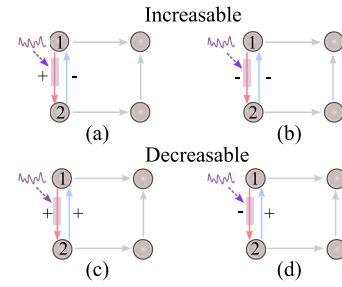


FIGURE 2. Illustration of vibrationally increasable and decreasable edges. (a) and (b): The red edge (i.e., (1,2)) is vibrationally increasable since the edge in the reverse direction has negative weight. (c) and (d): It is vibrationally decreasable since the reverse edge has positive weight. Injecting a vibration to the red edge itself can functionally increase or decrease its weight in the corresponding cases.

$\mathcal{E}_A : a_{ij} < 0\}$, and $\mathcal{E}_{\text{dec}} := \{(i, j) \in \mathcal{E}_A : a_{ij} > 0\}$, which are vibrationally increasable and decreasable edges, respectively. Subsequently, we define a directed and signed graph $\mathcal{G}_A^{\text{mod}} := (\mathcal{V}, \mathcal{E}_{\text{mod}}, S)$, where $\mathcal{E}_{\text{mod}} = \mathcal{E}_{\text{inc}} \cup \mathcal{E}_{\text{dec}}$, and $S = [s_{ij}]$ with $s_{ij} = -\text{sign}(a_{ij})$ if $(i, j) \in \mathcal{E}_A$ and $s_{ij} = 0$ otherwise. We refer to $\mathcal{G}_A^{\text{mod}}$ as the *modifiable graph* of \mathcal{G}_A . An example is shown in Fig. 4(b). Given a graph \mathcal{G}_Δ , we denote $\mathcal{G}_\Delta \subseteq \mathcal{G}_A^{\text{mod}}$ if the signed (but unweighted) edges of \mathcal{G}_Δ constitute a subset of $\mathcal{G}_A^{\text{mod}}$'s.

Theorem 2: Consider a matrix $\Delta = [d_{ij}] \in \mathbb{R}^{n \times n}$, and let $\mathcal{G}_\Delta := (\mathcal{V}, \mathcal{E}_\Delta, \Delta)$ be the directed and signed graph associated with it. If \mathcal{G}_Δ is a directed acyclic graph (i.e., a graph with no cycles) and $\mathcal{G}_\Delta \subseteq \mathcal{G}_A^{\text{mod}}$, there exist vibrational control inputs such that the system matrix \bar{A} of (28) becomes $\bar{A} = A + \Delta$. Further, if $A + \Delta$ is Hurwitz., there exist ε_0 such that, for any $\varepsilon < \varepsilon_0$, the system (27) is exponentially stable.

This theorem provides a method to functionally change the system matrix from A to $A + \Delta$, which stabilizes the system if $A + \Delta$ is Hurwitz. A matrix Δ , which is associated with an acyclic graph \mathcal{G}_Δ and $\mathcal{G}_\Delta \subseteq \mathcal{G}_A^{\text{mod}}$, is called as *realizable modification matrix*, and \mathcal{G}_Δ is called *realizable modification graph*, given that, under these conditions, there exist vibrational inputs to realize the desired functional changes. Next, we show how to design such control inputs.

By assumption, \mathcal{G}_Δ is directed acyclic, then, from [38], it can be topologically ordered. Therefore, there exists a permutation matrix Q such that the matrix $\Delta' := Q\Delta Q^{-1}$ is quasi-lower-triangular. One can let $A' = QAQ^{-1}$, and $U'(t)$ be the vibrational control matrix to A' . Let $x' = Qx$, one can derive that the controlled system becomes

$$\dot{x}' = \left(A' + \frac{1}{\varepsilon} U' \left(\frac{t}{\varepsilon} \right) \right) x'. \quad (30)$$

Now, to functionally change A to $A + \Delta$, it becomes to change A' to $A' + \Delta'$.

⁴We highlight that the terminology we employ here is different from *functional network* that is widely-used in neuroscience (e.g., see [37]). To avoid possible confusion, we clarify that, when we say that vibrational control functionally changes the network \mathcal{G}_A , we mean that it leads to a functioning network $\mathcal{G}_{\bar{A}}$ that is different from \mathcal{G}_A .

To realize this functional change, we consider the following vibrational control matrix that is quasi-lower-triangular:

$$U'(t) = \begin{bmatrix} 0 & 0 & 0 & \dots & 0 \\ u'_{21}(t) & 0 & 0 & \dots & 0 \\ u'_{31}(t) & u'_{32}(t) & 0 & \dots & 0 \\ \vdots & \vdots & \vdots & \ddots & \vdots \\ u'_{n1}(t) & u'_{n2}(t) & u'_{n3}(t) & \dots & 0 \end{bmatrix},$$

where $u'_{ij}(t) = u'_{ij} \sin(\beta'_{ij}t)$. Then, the state transition matrix of the system $\dot{\hat{x}} = U(t)\hat{x}$ has the following form:

$$\Phi'(t, t_0) = \begin{bmatrix} 1 & 0 & 0 & \dots & 0 \\ \phi'_{21}(t) & 1 & 0 & \dots & 0 \\ \phi'_{31}(t) & \phi'_{32}(t) & 1 & \dots & 0 \\ \vdots & \vdots & \vdots & \ddots & \vdots \\ \phi'_{n1}(t) & \phi'_{n2}(t) & \phi'_{n3}(t) & \dots & 1 \end{bmatrix}.$$

According to [30], the averaged system matrix of (30), denoted as $\dot{\bar{x}} = \bar{A}\bar{x}$, satisfies $\bar{A} = A' + \bar{B}$ with

$$\bar{B} = [\bar{b}_{ij}] = A'^{\top} \odot C. \quad (31)$$

Here, $C = [c_{ij}]$ satisfies

$$c_{ij} = -\frac{1}{T} \int_{t=0}^T (\phi'_{ij}(\tau))^2 dt. \quad (32)$$

We need to design vibrational control inputs such that $\bar{B} = \Delta$. In other words, one needs to design vibrations such that

$$c'_{ij} = -\frac{d'_{ij}}{a'_{ji}}, \text{ if } a'_{ji} \neq 0; c'_{ij} = 0, \text{ otherwise.} \quad (33)$$

One can derive that, for any $i \geq 2$,

$$\begin{aligned} \phi'_{i,i-1}(t) &= \int_{t_0}^t u'_{i,i-1}(\tau) d\tau \\ &= -\frac{u'_{i,i-1}}{\beta'_{i,i-1}} (\cos(\beta'_{i,i-1}t) - \cos(\beta'_{i,i-1}t_0)), \end{aligned} \quad (34)$$

$$\phi'_{ij}(t) = \int_{t_0}^t \sum_{k=1}^{i-1} u'_{ik}(\tau) \phi'_{kj}(\tau) d\tau, \text{ for } j \leq i-2. \quad (35)$$

Combining the expressions in (34) and (35) with (32), one can derive the required ratios of the amplitudes and frequencies, i.e., $\frac{u'_{ij}}{\beta'_{ij}}$, in $U'(t)$. First, for each $i \geq 2$, it follows from (34) and (32) that

$$\frac{u'_{i,i-1}}{\beta'_{i,i-1}} = \sqrt{2c'_{i,i-1}} = \sqrt{\frac{-2d'_{i,i-1}}{a'_{i-1,i}}}, \text{ if } a'_{i-1,i} \neq 0. \quad (36)$$

Next, one can establish the remaining parameters within the vibrational control matrix through a recursive method. To do this, one calculates the necessary ratio $\frac{u'_{ij}}{\beta'_{ij}}$ by systematically deriving each required ϕ'_{ij} in the sequence outlined in Fig. 3.

FIGURE 3. Vibtaional control design. We first design the ratio u'_{ij}/β'_{ij} in each vibrational input $u'_{ij}(t)$, which can be done by once $\phi'_{ij}(t)$ is derived. The entries that are one-element left to the diagonals of Φ' are expressed by (34), which leads to the corresponding ratios in (36). The remaining entries of Φ' can be determined one by one in the order depicted by the above arrows, which can also be used to determine the ratios. After all the ratios are determined, one can choose amplitudes and frequencies to satisfy the corresponding ratio.

Once the ratios $\frac{u'_{ij}}{\beta'_{ij}}$ have been determined, one can select amplitudes and frequencies to fulfill these ratios. Note that the frequencies β'_{ij} need to be incommensurable, that is, each $\beta'_{ij}/\beta'_{k\ell}$ for any distinct pair of $\{i, j\}$ and $\{k, \ell\}$ is not a rational number. Consequently, the vibrational control matrix $U'(t)$ is determined. Subsequently, as $A = Q^{-1}A'Q$, the vibrational control to the original system (27) becomes

$$U(t) = Q^{-1}U'(t)Q.$$

Remark 1: Theorem 2 also provides an approach to improve the robustness of the system by vibrational control. As illustrated in Fig. 4, if there is a matrix Δ satisfying the conditions (i)-(ii) and $\mathcal{R}(A + \Delta) > \mathcal{R}(A)$, one can follow the above steps to design vibrational inputs to realize this functional change. We wish to mention that it is likely impossible to improve the system to any desired robustness by just adding a matrix Δ , especially when Δ is constrained by the graph structure. There are some interesting open questions. For instance, what is the realizable range of robustness levels? How to design Δ and the subsequent vibrational control to realize a desired and reasonable robustness?

B. KURAMOTO-OSCILLATOR NETWORKS

Observe that, in each cluster, oscillators have an identical frequency, and each pair is coupled by bidirected edges with asymmetric strengths. To study how vibrational control can improve the robustness of synchronization in each cluster, we consider the following homogeneous Kuramoto model:

$$\dot{\varphi}_i = \omega + \sum_{j=1}^n w_{ij} \sin(\varphi_j - \varphi_i), \quad (37)$$

where $i = 1, \dots, n$, and w_{ij} 's describe the directed network $\mathbb{G} = (\mathbb{V}, \mathbb{E})$ with $|\mathbb{E}| = m$. Let $B \in \mathbb{R}^{n \times m}$ be the incidence matrix of \mathbb{G} . Select a directed spanning tree \mathbb{G}_{span} in \mathbb{G} , and let $\hat{B} \in \mathbb{R}^{n \times (n-1)}$ be its incidence matrix. Denote $\varphi = [\varphi_1, \dots, \varphi_m]$ and $W = \text{diag}([w_{ij}]_{(i,j) \in \mathbb{E}}) \in \mathbb{R}^{m \times m}$.

Let $x = \hat{B}^{\top} \varphi \in \mathbb{R}^{n-1}$, and following similar steps as Appendix A one can derive that

$$\dot{x} = -\hat{B}^{\top} B W \sin(R_1 x), \quad (38)$$

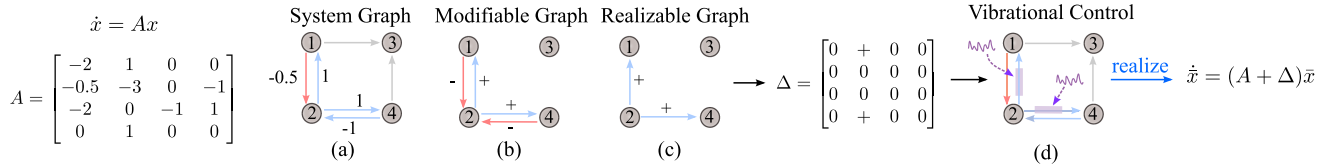


FIGURE 4. Illustration of the method to improve robustness of a linear stable system. (a) The directed graph associated with $\dot{x} = Ax$. (b) Modifiable graph, where edges can be vibrationally changed (the signs indicate whether they can be increased or decreased). (c)-(d) If a matrix Δ corresponds to a signed and directed graph that is directed acyclic and it is a subgraph of the modifiable graph, then there exists vibrational control to realize the averaged system $\dot{\bar{x}} = (A + \Delta)\bar{x}$. Careful design of Δ can increase the robustness of the original system.

where \mathbb{B} is obtained by replacing the negative elements in the oriented incidence matrix B with 0 and

$$R_1 = \begin{bmatrix} B^T (\hat{B}^T)^\dagger \\ -B^T (\hat{B}^T)^\dagger \end{bmatrix}.$$

With vibrations injected into the edges in the network, we have the controlled model

$$\dot{x} = -\hat{B}^T \mathbb{B} \left(\mathbf{W} + \frac{1}{\varepsilon} \mathbf{U} \left(\frac{t}{\varepsilon} \right) \right) \sin(R_1 x), \quad (39)$$

where $\mathbf{U}(t) = \text{diag}([u_{ij}]_{(j,i) \in \mathbb{E}}) \mathbb{R}^{m \times m}$. Linearizing the system (39) at $x = 0$, we obtain

$$\dot{x} = -\hat{B}^T \mathbb{B} \left(\mathbf{W} + \frac{1}{\varepsilon} \mathbf{U} \left(\frac{t}{\varepsilon} \right) \right) R_1 x. \quad (40)$$

Denote $J = -\hat{B}^T \mathbb{B} \mathbf{W} R_1$. Similar to the previous section, one can associate (40) with the following averaged system

$$\dot{\bar{x}} = \bar{J} \bar{x} \quad (41)$$

where

$$\bar{J} = \lim_{T \rightarrow \infty} \frac{1}{T} \int_{t=0}^T \Phi^{-1}(t, t_0) J \Phi(t, t_0) dt,$$

and $\Phi(t, t_0)$ is the state transition matrix of the system

$$\dot{z} = P(t)z, \text{ where } P(t) = -\hat{B}^T \mathbb{B} \mathbf{U}(t) R_1. \quad (42)$$

Due to the presence of the matrices \hat{B} , \mathbb{B} , and R_1 , $P(t)$ has a very complex dependence on the vibrations injected to the edges in the Kuramoto-oscillator network. As a consequence, it becomes very challenging to design vibrational control $\mathbf{U}(t)$ to modify the elements in J so that the robustness of synchronization can be improved.

Our goal is to provide a tractable and predictable approach to design vibrational control to improve the robustness of the synchronization by functionally modifying the elements in J . To this end, we will use the results we established for linear systems in Section V-A.

Specifically, our method consists of the following steps (an example is provided in Fig. 5 to illustrate the procedure).

- 1) First, selecting a \hat{B} we compute the Jacobian matrix J and associate it with a weighted directed graph \mathbb{G}_J .
- 2) Following the same steps in Section V-A, one can identify a modifiable graph from \mathbb{G}_J , denoted as $\mathbb{G}_J^{\text{mod}}$, containing increasable and decreasable edges in \mathbb{G}_J . Here, an edge (k, ℓ) is increasable (decreasable) if $j_{k\ell} <$

0 (resp., $j_{k\ell} > 0$). The definition here differs slightly from the one presented in the previous section. In linear network systems, an edge that does not exist is not considered part of the set of modifiable edges, as it cannot receive control inputs. However, in the linearized model of a Kuramoto network, a zero entry in the Jacobian matrix can still be influenced by vibrational control injected into the connections of the original Kuramoto network (an example is shown in Fig. 5(a)). Let A_{mod} be the unweighted adjacency matrix of \mathbb{G}_J .

- 3) We assume that $\mathbf{U}(t)$ contains non-zero values at all off-diagonal positions (we will gradually set them to 0 at positions that we do not intend to control). To assess how vibrations injected into the edges of the Kuramoto-oscillator network impact the edges within \mathbb{G}_J , we calculate $P(t) = -\hat{B}^T \mathbb{B} \mathbf{U}(t) R_1$. Since whether an edge in \mathbb{G}_J can be altered is determined by its modifiable graph, we let $P_1(t) = P(t) \odot (I + A_{\text{mod}})$. This operation retains only the elements corresponding to modifiable edges.
- 4) While configuring control inputs, one needs to deal with the situation that a vibration introduced to a single edge in the Kuramoto-oscillator network can bring changes to multiple edges in \mathbb{G}_J . To make the design procedure more analytically tractable, we remove the vibrations that appear two or more times in the off-diagonal positions in $P_1(t)$ and obtain $\hat{P}(t)$.
- 5) We associate $\hat{P}(t)$ with a directed graph $\mathbb{G}_{\hat{P}}$. Now, we configure vibrational control inputs such that $\mathbb{G}_{\hat{P}}$ does not contain a directed cycle (also no self-loops). Consequently, the resulting graph determines realizable changes to J that vibrations can bring in, which we refer to as a *realizable graph*. For any Δ , there always exists a vibrational control that functionally changes J to $\bar{J} = J + \Delta$ if the associated directed and sign graph of Δ is a realizable graph (see Fig. 5(c)). One can simply use the results in Section V-A to design vibrational inputs.

Remark 2: The vibrations that exclusively affect the diagonal positions of $P(t)$ play a crucial role in the design process. They are often utilized to counteract the impact of other vibrations on the diagonal, ensuring that they only influence a single off-diagonal element in $P(t)$. To maximize the occurrence of vibrations exclusively in the diagonal positions, an effective approach is to select a spanning tree with minimal

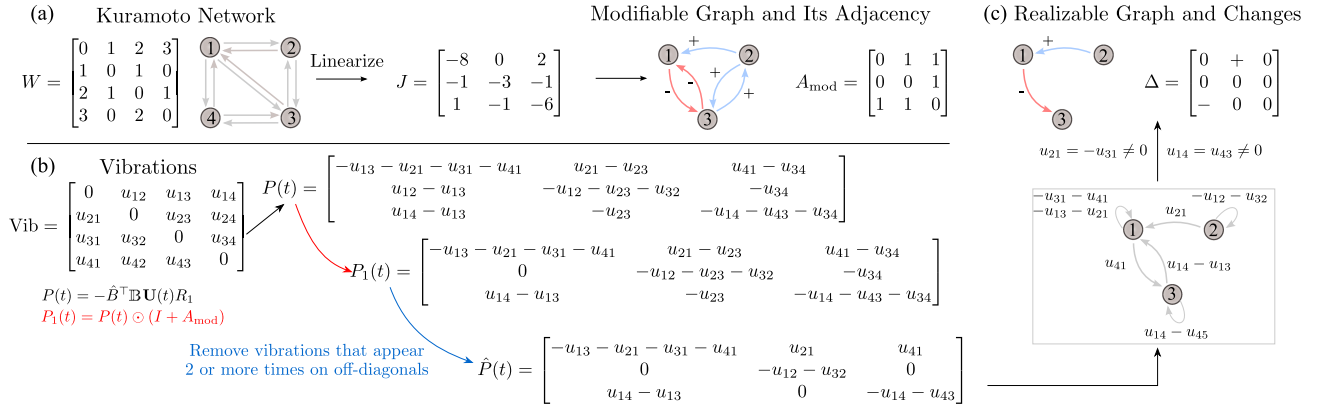


FIGURE 5. Illustration of making predictable changes in the Kuramoto-oscillator network. (a) One linearizes the Kuramoto model and obtain a linear system $\dot{x} = Jx$. Following the steps in Section V-A, a modifiable graph and its adjacency matrix can be found. (b) We investigate how vibrations in the Kuramoto-oscillator network influence the linearized system by computing $P = \hat{B}^T \mathbb{B} U(t) R_1$ (in the figure, the incidence matrix \hat{B} corresponds to the spanning tree consisting of the edges $\{(3, 1), (3, 2), (3, 4)\}$). From the modifiable graph in (a), we only keep elements in $P(t)$ that corresponds to modifiable edges, resulting in $P_1(t)$. Further, to make the design of vibrational control tractable, we remove the vibrations that appear two or more times in off-diagonal positions and obtain $\hat{P}(t)$. (c) We associate $\hat{P}(t)$ with a directed graph $\mathcal{G}_{\hat{P}}$ that allows for self-loops. Then, it remains to configure vibrations such that the directed graph has no directed cycles (including self-loops). For instance, one can set $u_{21}(t) = -u_{31}(t)$, $u_{14}(t) = u_{43}(t)$, and any other vibrations to zero to realize the changes indicated in the upper panel. Any change that has the same pattern as Δ can be realized by choosing the amplitudes and frequencies in the vibrations $u_{21}(t)$ and $u_{14}(t)$ following the steps in Section V-A.

depth to define \hat{B} . For example, in Fig. 5(a), one can opt for the spanning tree composed of edges $(3, 1)$, $(3, 2)$, $(3, 4)$. This choice facilitates the isolation of vibrations to the diagonal positions.

C. DESIGN OF VIBRATIONAL CONTROL FOR CLUSTER SYNCHRONIZATION STABILIZATION

Now, we can use the results in the previous section to design vibrations to stabilize cluster synchronization.

Recall that oscillators in each cluster have an identical frequency. Following the same procedure as in the previous section, one can identify a modifiable graph for each cluster, defining the edges that can be functionally modified via vibrational control. Denote the modifiable graphs by $\mathbb{G}_{\text{mod}}^{(1)}, \mathbb{G}_{\text{mod}}^{(2)}, \dots, \mathbb{G}_{\text{mod}}^{(r)}$.

Corollary 1: Consider matrices $\Delta^{(k)} \in \mathbb{R}^{n_k \times n_k}$, $k = 1, 2, \dots, r$, and let $\mathcal{G}_{\Delta^{(k)}}$ be the directed and signed graph associated with them. Assume that they satisfy the following conditions:

- i) Each $\mathcal{G}_{\Delta^{(k)}}$ is acyclic and satisfies $\mathcal{G}_{\Delta^{(k)}} \subseteq \mathbb{G}_{\text{mod}}^{(k)}$.
- ii) The matrix $S = [s_{k\ell}]_{r \times r}$ defined by

$$s_{k\ell} = \begin{cases} \mathcal{R}(J^{(k)} + \Delta^{(k)}) - \bar{\gamma}_{kk}, & \text{if } k = \ell, \\ -\bar{\gamma}_{k\ell}, & \text{if } k \neq \ell. \end{cases}$$

is an M -matrix.

Then, there exists $\varepsilon_0 > 0$ such that for any $\varepsilon < \varepsilon_0$, vibrational control inputs, which functionally change the Jacobian matrix $J^{(k)}$ in each cluster to $J^{(k)} + \Delta^{(k)}$, $k = 1, 2, \dots, r$, stabilize the cluster synchronization manifold \mathcal{M} .

We wish to mention that one can follow the same steps as in Sections V-A and V-B to design the amplitudes and frequencies of vibrational inputs.

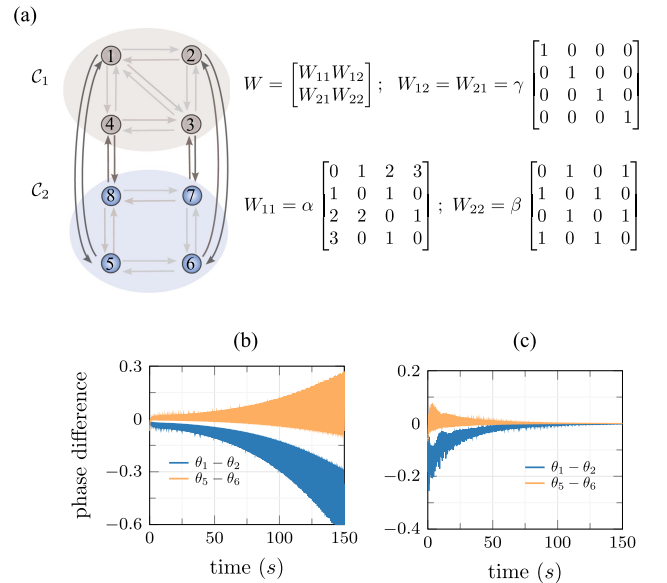


FIGURE 6. Vibrational stabilization of a cluster synchronization manifold. (a) The network structure and the connection weights, where $\alpha = 0.05$, $\beta = 1$, and $\gamma = 3$. (b) Phase differences without control, indicating that the cluster synchronization is unstable. (c) Phase differences under vibrational control to the cluster C_1 , showing that the cluster synchronization has been stabilized by local vibrations. The natural frequencies in C_1 and C_2 are $\omega_1 = 1$ and $\omega_2 = 10$, respectively.

VI. NUMERICAL STUDY

In this section, we employ an example to show how to design vibrations to stabilize cluster synchronization in a Kuramoto-oscillator network.

The network we consider is shown in Fig. 6(a). Partitioning the network into two clusters C_1 and C_2 , Assumption 1 is satisfied so that the corresponding cluster synchronization manifold \mathcal{M} is invariant. However, this pattern of cluster

synchronization is unstable (see in Fig. 6(b)). Then, we design a vibrational control to stabilize it.

We observe that the first cluster has the same network structure as that in Fig. 5. Within each cluster, one can derive that the linearized system $\dot{x}^{(k)} = J^{(k)}x^{(k)}$ has

$$J^{(1)} = \alpha \begin{bmatrix} -8 & 0 & 2 \\ -1 & -4 & -1 \\ 1 & -1 & -5 \end{bmatrix}, \quad J^{(2)} = \begin{bmatrix} -3 & 0 & 1 \\ -1 & -2 & 1 \\ 1 & 0 & -3 \end{bmatrix},$$

where $\alpha = 0.05$. Following the definition (24), one can compute that $\mathcal{R}(J^{(1)}) = 0.305$ and $\mathcal{R}(J^{(2)}) = 3.62$. One notices that the robustness of synchronization within \mathcal{C}_1 is very small. Therefore, our objective becomes to improve the robustness in \mathcal{C}_1 . Since cluster \mathcal{C}_1 share the same network structure as that in Fig. 5, we can use the realizable graphs and changes identified there. Particularly, we choose

$$\Delta^{(1)} = 0.05 \begin{bmatrix} 0 & 1 & 0 \\ 0 & 0 & 0 \\ -1 & 0 & 0 \end{bmatrix}$$

as the change we want to bring to \mathcal{C}_1 .

One can compute that this change improves the robustness from $\mathcal{R}(J^{(1)}) = 0.305$ to $\mathcal{R}(J^{(1)} + \Delta^{(1)}) = 0.332$.

Following the steps in Theorem 2, to realize the changes described by $\Delta^{(1)}$, we inject the vibrations below to the connections a_{21} , a_{31} , a_{14} , and a_{45} , respectively:

$$u_{21}(t) = -u_{31}(t) = \frac{k_1}{\varepsilon} \sin\left(\frac{\beta_1 t}{\varepsilon}\right),$$

$$u_{14}(t) = u_{45}(t) = \frac{k_2}{\varepsilon} \sin\left(\frac{\beta_2 t}{\varepsilon}\right),$$

where $\beta_1 = 1$, $\beta_2 = \sqrt{2}$, and

$$k_1 = \sqrt{-\frac{0.05}{J_{21}^{(1)}}}, \text{ and } k_2 = \sqrt{\frac{0.1}{J_{13}^{(1)}}}.$$

Now, according to Theorem 1, there exist a threshold for ε such that ε needs to be less than it. Yet, how to identify that threshold is still an open problem. In practice, one can simply try to choose a small ε . Fortunately, ε often does not need to be very small. For instance, as it is shown in Fig. 6, $\varepsilon = 0.01$ is sufficient to stabilize the cluster synchronization.

We wish to mention that the condition in Theorem 1 and Corollary 1 are not even satisfied. This indicates that the condition we have identified is still a bit conservative. More tight conditions call for future studies. However, it is worth highlighting the power of vibrational control since a slight improvement on the robustness effectively stabilizes the cluster synchronization.

VII. DISCUSSION

Cluster synchronization plays an very important role in many natural and man-made systems. Losing of stability of desired patterns of cluster synchronization often means malfunction. In this article, we study how vibrational control, an open-loop

control strategy, can be used to stabilize cluster synchronization. We construct some sufficient conditions under which a vibrational control stabilizes cluster synchronization. We show that one of the working mechanisms of vibrational control is that it improves the robustness of local synchronization within each cluster. Further, we provide a tractable approach to design vibrational control inputs. We utilize numerical experiments to validate our theoretical findings.

We conjecture that vibrational control can provide some interpretation of how deep brain stimulation works, which can potentially inform the design of better brain stimulation therapies. In the future, we are interested in extending the existing open-loop vibrational control strategy to closed-loop ones, even in the presence of imperfect measurement of system states. This hopefully would contribute to the design of better closed-loop deep brain stimulation.

APPENDIX

A. DERIVATION OF THE COMPACT SYSTEM

Without loss of generality, we arrange the columns in the incidence matrices, as defined in Section III-A, in a manner such that the intra-cluster edges within the subnetwork precede the inter-cluster edges. Mathematically, we have

$$B = [B_{\text{intra}}, B_{\text{inter}}], \quad B_{\text{intra}} = \text{blkdiag}(B_{\text{intra}}^{(1)}, \dots, B_{\text{intra}}^{(r)})$$

$$\hat{B} = [\hat{B}_{\text{intra}}, \hat{B}_{\text{inter}}], \quad \hat{B}_{\text{intra}} = \text{blkdiag}(\hat{B}_{\text{intra}}^{(1)}, \dots, \hat{B}_{\text{intra}}^{(r)}).$$

Recall that w_{ij} 's are the connection weights in the network \mathcal{G} . Now, we define the diagonal matrix consisting of these weights by

$$W = \begin{bmatrix} W_{\text{intra}} & 0 \\ 0 & W_{\text{inter}} \end{bmatrix} \in \mathbb{R}^{m \times m} \quad (43)$$

where $W_{\text{intra}} := \text{diag}\{w_{ij}, (i, j) \in \mathcal{E}_{\text{intra}}\}$ and $W_{\text{inter}} := \text{diag}\{w_{ij}, (i, j) \in \mathcal{E}_{\text{inter}}\}$ are also diagonal matrices, containing the weights of intra- and inter-cluster connections, respectively. Likewise, one can use

$$V(t) = \begin{bmatrix} V_{\text{intra}}(t) & 0 \\ 0 & V_{\text{inter}}(t) \end{bmatrix} \quad (44)$$

to denote the diagonal matrix that contains the vibrations injected to the corresponding edges in (43). Note that the bold notation \mathbf{W} and \mathbf{V} are different from W and V defined in Section 1; in fact, they are obtained by rewriting the non-zeros entries in W and V into a diagonal matrix, respectively. Now, one can rewrite the controlled system (6) into

$$\dot{\theta} = \omega - \mathbb{B}(\mathbf{W} + \mathbf{V}(t)) \sin(B^\top \theta), \quad (45)$$

where $\omega = [\omega_1, \omega_2, \dots, \omega_n]^\top$, \mathbb{B} is a matrix obtained by replacing the negative elements in the oriented incidence matrix B with 0. Likewise, we define $\mathbb{B}_{\text{intra}}$ and $\mathbb{B}_{\text{inter}}$, and then we have $\mathbb{B} = [\mathbb{B}_{\text{intra}}, \mathbb{B}_{\text{inter}}]$. Also, we write $\mathbb{B}_{\text{intra}} = [\mathbb{B}_{\text{intra}}^{(1)}, \mathbb{B}_{\text{intra}}^{(2)}, \dots, \mathbb{B}_{\text{intra}}^{(r)}]$.

Recall that $x = \hat{B}_{\text{intra}}^\top \theta$ and $y = \hat{B}_{\text{inter}}^\top \theta$. Then, it holds that

$$\dot{x} = -\hat{B}_{\text{intra}}^\top \mathbb{B}(\mathbf{W} + \mathbf{V}(t)) \sin(B^\top \theta), \quad (46a)$$

$$\dot{y} = \hat{B}_{\text{inter}}^\top \omega - \hat{B}_{\text{inter}}^\top \mathbb{B}(\mathbf{W} + \mathbf{V}(t)) \sin(B^\top \theta), \quad (46b)$$

where the fact that identical intra-cluster natural frequencies imply $\hat{B}_{\text{intra}}^\top \omega = 0$ has been used. Now, it remains to write $B^\top \theta$ into a function of x and y .

To this end, we provide the following instrumental lemma. Below, \bar{B} is the incidence matrix of the undirected counterpart of \mathcal{G} (replacing every pair of bidirectional edges with one undirected edge); and \bar{B}_{inter} and \bar{B}_{intra} are also the undirected counterparts of B_{inter} and B_{intra} , respectively. The matrix \bar{B}_{intra} can be decomposed with respect to different clusters as $\bar{B}_{\text{intra}} = [\bar{B}_{\text{intra}}^{(1)}, \dots, \bar{B}_{\text{intra}}^{(r)}]$. Also, we define two projection matrices

$$P_{\text{intra}} = I_n - \hat{B}_{\text{intra}} \hat{B}_{\text{intra}}^\dagger, P_{\text{inter}} = I_n - \hat{B}_{\text{inter}} \hat{B}_{\text{inter}}^\dagger,$$

where $(\cdot)^\dagger$ denotes the pseudo-inverse of a matrix.

Lemma 3: For the incidence matrices $B \in \mathbb{R}^{n \times m}$ and $\hat{B} \in \mathbb{R}^{n \times (n-1)}$ of the graph \mathcal{G} and its directed spanning tree $\hat{\mathcal{G}}$, there exists

$$R = \begin{bmatrix} R_1 & \mathbf{0} \\ R_2 & R_3 \end{bmatrix}$$

such that $B^\top = R\hat{B}^\top$, where

$$R_1 = \begin{bmatrix} R'_1 \\ -R'_1 \end{bmatrix}, R_2 = \begin{bmatrix} R'_2 \\ -R'_2 \end{bmatrix}, R_3 = \begin{bmatrix} R'_3 \\ -R'_3 \end{bmatrix},$$

with

$$\begin{aligned} R'_1 &= \bar{B}_{\text{intra}}^\top (\hat{B}_{\text{intra}}^\top P_{\text{inter}})^\dagger, \\ R'_2 &= \bar{B}_{\text{inter}}^\top (\hat{B}_{\text{intra}}^\top P_{\text{inter}})^\dagger, \\ R'_3 &= \bar{B}_{\text{inter}}^\top (\hat{B}_{\text{inter}}^\top P_{\text{intra}})^\dagger. \quad \Delta \end{aligned}$$

Proof: As \bar{B} is the incidence matrix of the undirected counterpart of \mathcal{G} , we can write

$$B = [\bar{B}_{\text{intra}}, -\bar{B}_{\text{intra}}, \bar{B}_{\text{inter}}, -\bar{B}_{\text{inter}}]. \quad (47)$$

The work [20] has shown that

$$\bar{B}^\top = \begin{bmatrix} \bar{B}_{\text{intra}}^\top \\ \bar{B}_{\text{inter}}^\top \end{bmatrix} = \begin{bmatrix} R'_1 & \mathbf{0} \\ R'_2 & R'_3 \end{bmatrix} \hat{B}^\top,$$

which means that

$$\bar{B}_{\text{intra}}^\top = R'_1 \hat{B}^\top, \text{ and } \bar{B}_{\text{inter}}^\top = R'_2 \hat{B}_{\text{intra}}^\top + R'_3 \hat{B}_{\text{inter}}^\top.$$

Substituting them into (47) completes the proof. \square

Applying Lemma 3 to (46), we obtain

$$B^\top \theta = \begin{bmatrix} R_1 & 0 \\ R_2 & R_3 \end{bmatrix} \hat{B}^\top \theta = \begin{bmatrix} R_1 & 0 \\ R_2 & R_3 \end{bmatrix} \begin{bmatrix} x \\ y \end{bmatrix}.$$

Subsequently, one can derive that the functions in the compact system (9) are given by

$$f_{\text{intra}}(x) = -\hat{B}_{\text{intra}}^\top \mathbb{B}_{\text{intra}} \mathbf{W}_{\text{intra}} \sin(R_1 x) \quad (48a)$$

$$f_{\text{inter}}(x, y) = -\hat{B}_{\text{inter}}^\top \mathbb{B}_{\text{inter}} \mathbf{W}_{\text{inter}} \sin(R_2 x + R_3 y) \quad (48b)$$

$$h_{\text{ctl}}(V(t), x, y) = -\hat{B}_{\text{intra}}^\top \mathbb{B}_{\text{intra}} \mathbf{V}_{\text{intra}}(t) \sin(R_1 x)$$

$$- \hat{B}_{\text{intra}}^\top \mathbb{B}_{\text{inter}} \mathbf{V}_{\text{inter}}(t) \sin(R_2 x + R_3 y), \quad (48c)$$

$$g(x, y) = \hat{B}_{\text{inter}}^\top \omega - \hat{B}_{\text{inter}}^\top \mathbb{B}_{\text{intra}} \mathbf{W}_{\text{intra}} \sin(R_1 x) \quad (48d)$$

$$- \hat{B}_{\text{inter}}^\top \mathbb{B}_{\text{inter}} \mathbf{W}_{\text{inter}} \sin(R_2 x + R_3 y) \quad (48e)$$

$$h'_{\text{ctl}}(V, x, y) = -\hat{B}_{\text{inter}}^\top \mathbb{B}_{\text{intra}} \mathbf{V}_{\text{intra}}(t) \sin(R_1 x)$$

$$- \hat{B}_{\text{inter}}^\top \mathbb{B}_{\text{inter}} \mathbf{V}_{\text{inter}}(t) \sin(R_2 x + R_3 y). \quad (48f)$$

Similar to $\mathbf{V}(t)$, one can define $\mathbf{U}(t) := \text{diag}(u_{ij}(t) : (i, j) \in \mathcal{E})$, and it follows that $\mathbf{V}(t) = \frac{1}{\varepsilon} \mathbf{U}(\frac{t}{\varepsilon})$. Then, (48) defines the functions in (9).

The function f_{intra} characterizes the inherent dynamics occurring within the clusters, while f_{inter} accounts for the dynamics resulting from the inter-cluster connections. The functions h_{ctl} and h'_{ctl} delineate the impact on the dynamics introduced by the vibrational control inputs.

In this article, we specifically investigate a form of vibrational control where vibrations are only introduced to the intra-cluster connections. Then, we have $\mathbf{V}_{\text{inter}}(t) = 0$. As a consequence,

$$h_{\text{ctl}}(V(t), x, y) = \hat{B}_{\text{intra}}^\top \mathbb{B}_{\text{intra}} \mathbf{V}_{\text{intra}}(t) \sin(R_1 x),$$

$$h'_{\text{ctl}}(V, x, y) = -\hat{B}_{\text{inter}}^\top \mathbb{B}_{\text{intra}} \mathbf{V}_{\text{intra}}(t) \sin(R_1 x),$$

which no longer depend on y . Therefore, we denote them as $h_{\text{ctl}}(V(t), x)$ and $h'_{\text{ctl}}(V(t), x)$ for notational simplicity.

B. PROOF OF LEMMA 1

Since $x = 0$ is exponentially stable uniformly in y for the system (14), according to the converse Lyapunov theorem (see [32, Th. 4.4] and [39]) there exists $\mathcal{D} = \{\bar{x} \in \mathbb{R}^{n-r} : \|\bar{x}\| \leq \rho_1\}$ and a continuously differentiable function $V : [0, \infty) \times \mathcal{D} \times \mathbb{R}^r \rightarrow \mathbb{R}$ such that

$$\frac{\partial V}{\partial t} + \frac{\partial V}{\partial \bar{x}} ((J + P(t))\bar{x} + N(y)\bar{x}) \leq -c_1 \|\bar{x}\|^2$$

and $\|\frac{\partial V}{\partial \bar{x}}\| \leq c_2 \|\bar{x}\|$ for some constants $c_1, c_2 > 0$. Let

$$h(t, x) = f_{\text{intra}}(x) + f_{\text{ctl}}(U(t), x) + f_{\text{inter}}(x, y)$$

and $\Delta(t, x) = h(t, x) - (J + P(t))x - N(y)x$. It can be checked that $\partial h / \partial x$ is bounded and Lipschitz on \mathcal{D} . Then, similar to the proof of [40, Th. 4.13], one can show that $\|\Delta(t, x)\| \leq c_3 \|x\|^2$ for some $c_3 > 0$. The time derivative along the system (9) satisfies

$$\begin{aligned} \frac{\partial V}{\partial t} + \frac{\partial V}{\partial x} ((J + P(t) + N(y))x + \Delta(t, x)) \\ \leq -c_1 \|x\|^2 + c_2 c_3 \|x\|^3 \\ \leq -(c_1 - c_2 c_3 \rho) \|x\|^2, \forall \|x\| < \rho. \end{aligned}$$

Choosing $\rho = \min\{\rho_1, c_1/c_2 c_3\}$ completes the proof.

C. PROOF OF LEMMA 2

To construct the proof, one just needs to find vibrational control inputs that increase/decrease the weight of the edge (i, j) functionally in both situations.

Consider a vibrational control that is only injected to the edge (i, j) , i.e., $V(t)$ in (27) satisfies $v_{pq}(t) = 0$ for any $(p, q) \neq (i, j)$ and $V_{ji}(t) \neq 0$. One can label the nodes in the expanded network \mathcal{G} such that $i = 1$ and $j = n$. Then, the vibrational control matrix becomes

$$V(t) = \begin{bmatrix} 0 & 0 & \cdots & 0 \\ 0 & 0 & \cdots & 0 \\ \vdots & \vdots & \ddots & \vdots \\ v_{n1}(t) & 0 & 0 & 0 \end{bmatrix},$$

which has a quasi-lower-triangular form. Following the steps in [30], one can derive that \bar{A} in the averaged system (28) is

$$\bar{A} = A + \bar{B}, \text{ where } \bar{B} = \begin{bmatrix} 0 & 0 & \cdots & 0 \\ 0 & 0 & \cdots & 0 \\ \vdots & \vdots & \ddots & \vdots \\ b_{n1}(t) & 0 & 0 & 0 \end{bmatrix},$$

where $b_{n1} = -a_{1n} \lim_{T \rightarrow \infty} \frac{1}{T} \int_{t=0}^T F_{n1}^2(t) dt$ with $F_{n1}(t) = \int_0^t v_{n1}(\tau) d\tau$. If the edge $(n, 1)$ has a positive weight, i.e., $a_{1n} > 0$, $b_{n1} < 0$. If $a_{1n} < 0$, we have $b_{n1} > 0$, which completes the proof.

D. PROOF OF THEOREM 1

One can observe that (i) implies (ii). Then, it suffices to prove the exponential stability of $x = 0$ for (16). To do that, we first present the following lemma.

Lemma 4 (Growth bound of perturbations): There exist some constants $\bar{\gamma}_{k\ell} > 0$, $k, \ell = 1, \dots, r$, such that, for any k , it holds that $\|G^{(k)}(y)z\| \leq \sum_{\ell=1}^r \bar{\gamma}_{k\ell} \|z_\ell\| \cdot \Delta$.

Proof: To construct the proof, we write $N(y)$ into a block-diagonal form

$$N(y) = \begin{bmatrix} N^{11}(y) & \cdots & N^{1r}(y) \\ \vdots & \ddots & \vdots \\ N^{r1}(y) & \cdots & N^{rr}(y) \end{bmatrix},$$

where each $N^{ii}(y) \in \mathbb{R}^{(n_i-1) \times (n_i-1)}$. Then, it follows that

$$G^{(k)}(y)z = \sum_{\ell=1}^r (\Phi^{-1})^{(k)} N^{(k\ell)}(y) \Phi^{(\ell)} z_\ell.$$

Recall that Φ and Φ^{-1} are almost periodic, $\|\Phi\|$ and $\|\Phi^{-1}\|$ are both bounded. Let $c = \max_{k,\ell} \|(\Phi^{-1})^{(k)}\| \cdot \|\Phi^{(\ell)}\|$. Then, one can derive that

$$\|G^{(k)}(y)z\| \leq c \sum_{\ell=1}^r \|N^{(k\ell)}(y)z_\ell\| \leq c \sum_{\ell=1}^r \|N^{(k\ell)}(y)\| \|z_\ell\|.$$

Now, it remains to bound $\|N^{(k\ell)}(y)\|$. Recall that $N(y)$ is given by

$$N(y) = -(\hat{B}_{\text{intra}})^\top \mathbb{B}_{\text{inter}} W_{\text{inter}} (\mathbb{1}_{r-1} \otimes \sin(R_3 y)) \odot R_2.$$

Since $\sin(R_3)y$ is bounded independent of y , there exists a constant $c_{k\ell}$ such that $\|N^{(k\ell)}(y)\| \leq c_{k\ell}$. Letting $\bar{\gamma}_{k\ell} = cc_{k\ell}$ completes the proof. \square

Let $V_k = z_k^\top \bar{X}_k z_k$, and we have

$$\|\partial V_k / \partial z_k\| \leq \lambda_{\max}(\bar{X}_k) \|z_k\|.$$

Choose $V(z) = \sum_{k=1}^r d_k V_k$ as a Lyapunov candidate. The time derivative of $V(z)$ satisfies

$$\begin{aligned} \dot{V}(z) &= \sum_{k=1}^r d_k [z_k^\top ((\bar{J}^{(k)})^\top \bar{X}_k + \bar{X}_k \bar{J}^{(k)}) z_k \\ &\quad + \frac{\partial V}{\partial z_k} \Phi^{-1} N(y) \Phi z_k] \\ &\leq \sum_{k=1}^r d_k [-\|z_k\|^2 + \lambda_{\max}(\bar{X}_k) \sum_{\ell=1}^r \bar{\gamma}_{k\ell} \|z_k\| \|z_\ell\|], \end{aligned}$$

where the inequality has used Lemma 4.

Let $D := \text{diag}(d_1, \dots, d_r)$ and $\hat{S} = [\hat{s}_{ij}]_{r \times r}$ where

$$\hat{s}_{k\ell} = \begin{cases} 1 - \lambda_{\max}(\bar{X}_k) \bar{\gamma}_{k\ell}, & \text{if } k = \ell, \\ -\lambda_{\max}(\bar{X}_k) \bar{\gamma}_{k\ell}, & \text{if } k \neq \ell. \end{cases}$$

Then, one can rewrite $\dot{V}(z) \leq -\frac{1}{2} z^\top (DS + S^\top D)z$. By assumption, S is an M -matrix, and so is \hat{S} since $\hat{S} = S \cdot \text{diag}(\lambda_{\max}(\bar{X}_1), \dots, \lambda_{\max}(\bar{X}_r))$. It follows from [40, Th. 9.2] that the system (19) is exponentially stable.

Following similar steps as in [40, Th. 10.4], one can prove that there exists $\varepsilon^* > 0$ such that for any $\varepsilon < \varepsilon^*$, $z = 0$ is exponentially stable uniformly in y for the system (18). Since $x(s) = \Phi(s, s_0)z(s)$ and $\|\Phi\|$ is bounded, then $x = 0$ is also exponentially stable uniformly in y for (16), which completes the proof.

REFERENCES

- [1] G. Hahn, A. Ponce-Alvarez, G. Deco, A. Aertsen, and A. Kumar, "Portraits of communication in neuronal networks," *Nature Rev. Neurosci.*, vol. 20, no. 2, pp. 117–127, 2019.
- [2] J. Fell and N. Axmacher, "The role of phase synchronization in memory processes," *Nature Rev. Neurosci.*, vol. 12, no. 2, pp. 105–118, 2011.
- [3] C. Hammond, H. Bergman, and P. Brown, "Pathological synchronization in Parkinson's disease: Networks, models and treatments," *Trends Neurosciences*, vol. 30, no. 7, pp. 357–364, 2007.
- [4] P. Jiruska et al., "Synchronization and desynchronization in epilepsy: Controversies and hypotheses," *J. Physiol.*, vol. 591, no. 4, pp. 787–797, 2013.
- [5] R. E. Bellman, J. Bentsman, and S. M. Meerkov, "Vibrational control of nonlinear systems: Vibrational controllability and transient behavior," *IEEE Trans. Autom. Control*, vol. 31, no. 8, pp. 717–724, Aug. 1986.
- [6] B. Shapiro and B. T. Zinn, "High-frequency nonlinear vibrational control," *IEEE Trans. Autom. Control*, vol. 42, no. 1, pp. 83–90, Jan. 1997.
- [7] X. Cheng, Y. Tan, and I. Mareels, "On robustness analysis of linear vibrational control systems," *Automatica*, vol. 87, pp. 202–209, 2018.
- [8] J. K. Krauss et al., "Technology of deep brain stimulation: Current status and future directions," *Nature Rev. Neurol.*, vol. 17, no. 2, pp. 75–87, 2021.
- [9] T. Menara, G. Baggio, D. S. Bassett, and F. Pasqualetti, "Stability conditions for cluster synchronization in networks of heterogeneous Kuramoto oscillators," *IEEE Trans. Control Netw. Syst.*, vol. 7, no. 1, pp. 302–314, Mar. 2020.
- [10] T. Menara, G. Baggio, D. S. Bassett, and F. Pasqualetti, "A framework to control functional connectivity in the human brain," in *Proc. IEEE Conf. Decis. Control*, 2019, pp. 4697–4704.

- [11] T. Menara, G. Baggio, D. S. Bassett, and F. Pasqualetti, "Functional control of oscillator networks," *Nature Commun.*, vol. 13, 2022, Art. no. 4721.
- [12] L. M. Pecora, F. Sorrentino, A. M. Hagerstrom, T. E. Murphy, and R. Roy, "Cluster synchronization and isolated desynchronization in complex networks with symmetries," *Nature Commun.*, vol. 5, no. 1, 2014, Art. no. 4079.
- [13] Y. S. Cho, T. Nishikawa, and A. E. Motter, "Stable chimeras and independently synchronizable clusters," *Phys. Rev. Lett.*, vol. 119, no. 8, 2017, Art. no. 084101.
- [14] Y. Qin, M. Cao, B. D. O. Anderson, D. S. Bassett, and F. Pasqualetti, "Mediated remote synchronization: The number of mediators matters," *IEEE Control Syst. Lett.*, vol. 5, no. 3, pp. 767–772, Jul. 2021.
- [15] J. Emenheiser, A. Salova, J. Snyder, J. P. Crutchfield, and R. M. D'Souza, "Network and phase symmetries reveal that amplitude dynamics stabilize decoupled oscillator clusters," 2020, *arXiv:2010.09131*.
- [16] M. T. Schaub, N. O'Clery, Y. N. Billeh, J.-C. Delvenne, R. Lambiotte, and M. Barahona, "Graph partitions and cluster synchronization in networks of oscillators," *Chaos*, vol. 26, no. 9, 2016, Art. no. 094821.
- [17] Y. Qin, Y. Kawano, O. Portoles, and M. Cao, "Partial phase cohesiveness in networks of networks of Kuramoto oscillators," *IEEE Trans. Autom. Control*, vol. 66, no. 12, pp. 6100–6107, Dec. 2021.
- [18] P. Feketa, A. Schaum, and T. Meurer, "Stability of cluster formations in adaptive Kuramoto networks," *IFAC-PapersOnLine*, vol. 54, no. 9, pp. 14–19, 2021.
- [19] P. Feketa, A. Schaum, and T. Meurer, "Synchronization and multicluster capabilities of oscillatory networks with adaptive coupling," *IEEE Trans. Autom. Control*, vol. 66, no. 7, pp. 3084–3096, Jul. 2021.
- [20] R. Kato and H. Ishii, "Averaging and cluster synchronization of Kuramoto oscillators," in *Proc. Eur. Control Conf.*, 2021, pp. 1497–1502.
- [21] A. Salova and R. M. D'Souza, "Cluster synchronization on hypergraphs," 2021, *arXiv:2101.05464*.
- [22] A. Salova and R. M. D'Souza, "Analyzing states beyond full synchronization on hypergraphs requires methods beyond projected networks," 2021, *arXiv:2107.13712*.
- [23] W. Wu, W. Zhou, and T. Chen, "Cluster synchronization of linearly coupled complex networks under pinning control," *IEEE Trans. Circuits Syst.*, vol. 56, no. 4, pp. 829–839, Apr. 2009.
- [24] L. V. Gambuzza, M. Frasca, and V. Latora, "Distributed control of synchronization of a group of network nodes," *IEEE Trans. Autom. Control*, vol. 64, no. 1, pp. 365–372, Jan. 2019.
- [25] D. Fiore, G. Russo, and M. di Bernardo, "Exploiting nodes symmetries to control synchronization and consensus patterns in multiagent systems," *Control Syst. Lett.*, vol. 1, no. 2, pp. 364–369, 2017.
- [26] A. Allibhoy, F. Celi, F. Pasqualetti, and J. Cortés, "Optimal network interventions to control the spreading of oscillations," *IEEE Open J. Control Syst.*, vol. 1, pp. 141–151, 2022.
- [27] Y. Qin, D. S. Bassett, and F. Pasqualetti, "Vibrational control of cluster synchronization: Connections with deep brain stimulation," in *Proc. IEEE 61st Conf. Decis. Control*, 2022, pp. 655–661.
- [28] L. Tiberi, C. Favaretto, M. Innocenti, D. S. Bassett, and F. Pasqualetti, "Synchronization patterns in networks of Kuramoto oscillators: A geometric approach for analysis and control," in *Proc. IEEE 56th Annu. Conf. Decis. Control*, 2017, pp. 481–486.
- [29] R. E. Bellman, J. Bentsman, and S. M. Meerkov, "Vibrational control of nonlinear systems: Vibrational stabilization," *IEEE Trans. Autom. Control*, vol. 31, no. 8, pp. 710–716, Aug. 1986.
- [30] S. M. Meerkov, "Principle of vibrational control: Theory and applications," *IEEE Trans. Autom. Control*, vol. 25, no. 4, pp. 755–762, Aug. 1980.
- [31] M. H. Histed, V. Bonin, and R. C. Reid, "Direct activation of sparse, distributed populations of cortical neurons by electrical microstimulation," *Neuron*, vol. 63, no. 4, pp. 508–522, 2009.
- [32] W. M. Haddad and V. Chellaboina, *Nonlinear Dynamical Systems and Control: A Lyapunov-Based Approach*. Princeton, NJ, USA: Princeton Univ. Press, 2011.
- [33] J. A. Sanders, F. Verhulst, and J. Murdock, *Averaging Methods in Nonlinear Dynamical Systems*. New York, NY, USA: Springer, 2007.
- [34] R. A. Horn and C. R. Johnson, *Topics in Matrix Analysis*. Cambridge, U.K.: Cambridge Univ. Press, 1994.
- [35] H. G. Chen and K. W. Han, "Improved quantitative measures of robustness for multivariable systems," *IEEE Trans. Autom. Control*, vol. 39, no. 4, pp. 807–810, 1994.
- [36] R. Yedavalli, "Improved measures of stability robustness for linear state space models," *IEEE Trans. Automat. Control*, vol. 30, no. 6, pp. 577–579, Jun. 1985.
- [37] D. S. Bassett, A. Meyer-Lindenberg, S. Achard, T. Duke, and E. Bullmore, "Adaptive reconfiguration of fractal small-world human brain functional networks," *Proc. Nat. Acad. Sci.*, vol. 103, no. 51, pp. 19518–19523, 2006.
- [38] J. Bang-Jensen and G. Gutin, *Digraphs: Theory, Algorithms and Applications* (Monographs in Mathematics Series). London: Springer, 2000.
- [39] Y. Qin, Y. Kawano, B. D. Anderson, and M. Cao, "Partial exponential stability analysis of slow-fast systems via periodic averaging," *IEEE Trans. Automat. Control*, vol. 67, no. 10, pp. 5479–5486, Oct. 2022.
- [40] H. K. Khalil, *Nonlinear Systems*. Upper Saddle River, NJ, USA: Prentice Hall, 2002.



YUZHEN QIN (Member, IEEE) received the B. E. degree in control engineering from Hohai University, Nanjing, China, in 2012, the M. E. degree in control engineering from Wuhan University, Wuhan, China, in 2015, and the Ph.D. degree in systems and control from Engineering and Technology Institute (ENTEG), University of Groningen, Groningen, the Netherlands, in 2019. From 2020 to 2023, he was a Postdoctoral Researcher with the University of California, Riverside, CA, USA. He currently holds a tenure-track position with Radboud University, Nijmegen, the Netherlands. His research interests mainly include the areas of nonlinear network control system, network neuroscience, and reinforcement learning theory.



ALBERTO MARIA NOBILI received the B.Sc. degree in computer engineering and the M.Sc. degree in automation and robotics engineering from University of Pisa, Pisa, Italy, in 2019 and 2022, respectively. He is currently working toward the Ph.D. degree with the Institute of Mechanical Intelligence, Scuola Superiore Sant'Anna, Pisa, Italy. His research interests include control of network systems on one hand and of robotic exoskeletons on the other.



DANIELLE S. BASSETT (Member, IEEE) received the B.S. degree in physics from Penn State University, State College, PA, USA, and the Ph.D. degree in physics from the University of Cambridge, Cambridge, U.K., as a Churchill Scholar and as an NIH Health Sciences Scholar. They are currently the J. Peter Skirkanich Professor with the Departments of Bioengineering, Electrical & Systems Engineering, Physics & Astronomy, Neurology, and Psychiatry, University of Pennsylvania, Philadelphia, PA, USA. They are also an External

Professor with Santa Fe Institute, Santa Fe, NM, USA. They are most well-known for blending neural and systems engineering to identify fundamental mechanisms of cognition and disease in human brain networks. Following a Postdoctoral position with UC Santa Barbara, Santa Barbara, CA, USA, they were a Junior Research Fellow with the Sage Center for the Study of Mind. They are the author of more than 400 peer-reviewed publications, which have garnered more than 47 000 citations (h-index 101), as well as numerous book chapters and teaching materials. Their work has been supported by the National Science Foundation, National Institutes of Health, Army Research Office, Army Research Laboratory, Office of Naval Research, Department of Defense, Alfred P. Sloan Foundation, John D. and Catherine T. MacArthur Foundation, Paul Allen Foundation, ISI Foundation, and Center for Curiosity. They have recently co-authored *Curious Minds: The Power of Connection* (MIT Press) with philosopher and twin Perry Zurn. They were the recipient of multiple prestigious awards, including American Psychological Association's "Rising Star" (2012), Alfred P. Sloan Research Fellow (2014), MacArthur Fellow Genius Grant (2014), Early Academic Achievement Award from IEEE Engineering in Medicine and Biology Society (2015), Office of Naval Research Young Investigator (2015), National Science Foundation CAREER (2016), Popular Science Brilliant 10 (2016), Lagrange Prize in Complex Systems Science (2017), Erdos-Renyi Prize in Network Science (2018), OHBM Young Investigator Award (2020), AIMBE College of Fellows (2020), American Physical Society Fellow (2021), and has been named one of Web of Science's most Highly Cited Researchers for three years running.



FABIO PASQUALETTI (Member, IEEE) received the Laurea degree (B.Sc. equivalent) in computer engineering, the Laurea Magistrale degree (M.Sc. equivalent) in automation engineering from the University of Pisa, Italy, in 2004 and 2007, respectively, and the Ph.D. degree in mechanical engineering from the University of California, Santa Barbara, CA, USA, in 2012. He is currently a Professor of mechanical engineering with the University of California, Riverside, CA, USA. His research interests mainly include the analysis and

control of network systems, security of cyber-physical systems, and network neuroscience. He has received several awards, including a Young Investigator Research Program Award from AFOSR in 2020, Young Investigator Program Award from ARO in 2017, and the 2016 TCNS Outstanding Paper Award from IEEE CSS. He is the Member of SIAM.